Geophysica (2009), 45(1–2), 119–146

Finnish contribution to the Arctic Summer Cloud Ocean Study (ASCOS) expedition, Arctic Ocean 2008

Jussi Paatero[1], Petri Vaattovaara[2], Mika Vestenius[1], Outi Meinander[1], Ulla Makkonen[1], Rigel Kivi[1], Antti Hyvärinen[1], Eija Asmi[1], Michael Tjernström[3] and Caroline Leck[3]

[1]Finnish Meteorological Institute, Finland
[2]Department of Physics, University of Kuopio, Finland
[3]Department of Meteorology, Stockholm University, Sweden

(Received: April 2009; Accepted: September 2009)

Abstract

The Arctic Summer Cloud Ocean Study, ASCOS, was a six-week expedition in August-September 2008 north of the 87th latitude onboard the Swedish icebreaker Oden. The expedition was a contribution to the International Polar Year 2007/2008. ASCOS studies some of the controlling factors of the low-level cloud system, especially the formation of cloud condensation and ice nuclei, over the Arctic pack ice. This will improve the accuracy of the climate models in the Arctic area where the climate is expected to change faster than in any other part of the world.

A distinct feature of ASCOS is its necessarily interdisciplinary nature, which includes physical oceanography, marine and sea ice biogeochemistry, surface microlayer chemistry, aerosol, gas-phase and cloud chemistry and physics, and meteorology.

The expedition sailed from Longyearbyen, Svalbard, in the beginning of August. After a week's cruise the icebreaker was moored to a several square kilometres wide ice floe north of the 87th latitude. The ship was drifting with the ice floe for a month before the return voyage to Svalbard in the early September.

The Finnish contribution to the experimental part of ASCOS consisted of researchers and instruments from the Finnish Meteorological Institute (FMI) and the University of Kuopio (UKu). The FMI's measurement programme consisted of meteorology, ozone and radioactivity soundings, a UV radiation sensor, a visibility meter, a ceilometer, filter sampling for radionuclide, heavy metal and PAH analyses, canister sampling for VOC analyses, fog droplet and aerosol particle size distribution measurements, an ozone monitor, and a sea water bubble camera. The UKu measurement programme consisted of ultrafine particles organic fraction measurements.

Key words: Arctic Ocean, climate change, cloud properties, air chemistry

1. Introduction

The Arctic Summer Cloud Ocean Study, ASCOS, is an Arctic research project with its field phase based on a Swedish icebreaker expedition during the summer of 2008. The ASCOS expedition was the fourth expedition heading north of the 85th latitude with previous ones in 1991, 1996 and 2001 (*Leck et al*., 1996; *Leck et al*., 2001; *Leck et al*., 2004). The project contributes to the International Polar Year 2007/2008 (IPY) coordinated by the World Meteorological Organization (WMO) and the Interna-

tional Council of Science (ICSU). The ultimate objective of ASCOS is to understand processes that are poorly described in current climate models, in order to reduce the large uncertainty in projections of future Arctic climate (*ACIA*, 2004). Model simulations of Arctic clouds are particularly deficient, impeding correctly simulated radiative fluxes, vital for the snow/ice-albedo feedback *(Intrieri et al*., 2002a; *Intrieri et al*., 2002b; *Tjernström*, 2005; *Tjernström et al*., 2008; *Uttal et al*., 2002). ASCOS aims to improve the understanding of processes that control the evolution of clouds over the Arctic pack ice area, with an integrated study from the sea-ice interface to the cloud-topped atmospheric boundary layer (ABL). The lead partner of ASCOS is the Department of Meteorology of the Stockholm University (MISU). The logistical support was provided by the Swedish Polar Research Secretariat.

The necessary interdisciplinary scientific approach of ASCOS includes marine biochemistry, physical oceanography, aerosol, gas-phase and cloud chemistry and physics, and meteorology. Most of the ASCOS expedition time concentrated on an ice-drift operation when the icebreaker was moored to an ice floe, starting near the North Pole and drifting passively during the biologically most active period and into autumn freeze-up conditions from early August to mid-September. Ground-based remote sensing instruments provided continuous measurements of boundary-layer and cloud structure, while in-situ instruments on the ice and on the ship, and vertical profiling provided detailed process oriented information on boundary layer dynamics, atmospheric aerosol/cloud evolution, gas-phase chemistry and ocean/ice biochemistry. Instruments were deployed both onboard the icebreaker and on the ice. Detailed aerosol, cloud and meteorological profilings were conducted with helicopter measurements and radiosoundings. Complementary measurements were performed on a NASA DC-8 research aircraft flying from Kiruna, northern Sweden. The aims of ASCOS are:

- To determine the atmospheric processes that control boundary layer clouds north of 80°N
- To determine the evolution of cloud condensation (CCN) and ice forming nuclei (IFN)
- To determine the role of boundary-layer turbulence and surface properties for the exchange of heat, water, momentum and aerosols between the ocean/ice/air interface and with the troposphere
- To determine the role of marine biochemical processes for CCN and IFN formation, with emphasis on the open lead surface microlayer
- To test and implement reliable satellite algorithms for area-covering climate monitoring
- To provide a high-Arctic mirror-station of intense atmospheric measurements that for a limited time will sample data similar to monitoring stations around the rim of the Arctic Ocean, for example at Pallas-Sodankylä, northern Finland, Barrow, Alaska and Alert/Eureka, Canada
- To contribute to the data archive over the central Arctic Ocean collected during IPY

- To provide a comprehensive data set on the high Arctic climate system, for developing and testing of integrated climate models

The Finnish contribution to the experimental part of ASCOS consisted of researchers and instruments from the Finnish Meteorological Institute (FMI) and the University of Kuopio (UKu). Technical details of these measurements and some preliminary results on atmospheric aerosol particles together with aerosol-bound trace components and stratospheric ozone and UV radiation are presented in the following.

2. *Expedition platform and route*

ASCOS was based on the Swedish icebreaker Oden. The ship is owned and operated by the Swedish Maritime Administration. The ship was designed for both escort ice-breaking and for polar research operations and delivered in 1988. The overall length of the ship is 107.8 m and her displacement is 11000–13000 tons. There are accommodations for up to 80 people onboard.

The expedition departed from Longyearbyen, Svalbard 02 August 2008 onboard the icebreaker Oden. After leaving Isfjord, where Longyearbyen is located, the ship sailed westwards through the open water area (OW) and then northwards through the marginal ice zone (MIZ) stopping for 12 or 24 hours to have OW and MIZ research stations (Fig. 1). Then the ship sailed through the pack ice zone (PIZ) to just north of the 87th latitude where she was moored to an ice floe on 12 August 2008. The ice floe had

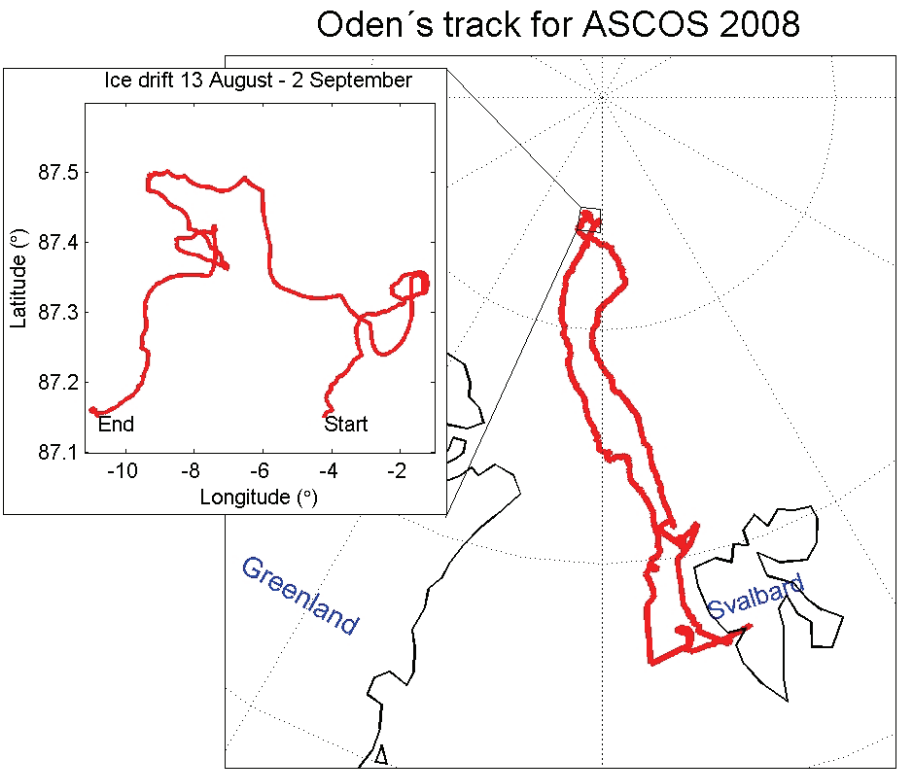

Fig. 1. Route of the ASCOS expedition in 2008.

an area of several square kilometres. Several measurement sites were established on the ice floe. The ship and the ice camp were drifting with the ice reaching 87º30'N, i.e. 150 nautical miles south of the North Pole. Oden headed south 02 September 2008 having additional research stations in the MIZ and in OW north-west of Spitzbergen. She arrived back to Longyearbyen 09 September 2008.

3. Materials and methods

3.1 Measurement and sampling programme

The Finnish Meteorological Institute's contribution to the ASCOS measurement and sampling programme consisted of over a dozen of different parameters:

- Eight ozone soundings were performed using Vaisala RS92 sondes with electrochemical ozone sensors and a DigiCORA III sounding processor,
- Six radioactivity soundings were made using Vaisala RS92 sondes with radioactivity sensors equipped with two geiger-müller tubes and a DigiCORA III sounding processor,
- Ultraviolet radiation was measured with a NILU-UV multibandfilterradiometer (MBFR, NILU Products AS). The instrument has five channels with nominal center wavelengths at 305, 313, 320, 340, 380 nm, and an additional channel (400–700 nm) for the measurment of photosynthetically active radiation,
- Cloud base height up to 8 kilometres and cloud coverage was measured with a Vaisala CT25K laser ceilometer,
- Vaisala present weather sensor FD12P consisting of a rain detector and a visibility meter produced present weather SYNOP codes, cloud data and visibility data,
- Fog droplet particle number concentration and size distribution between 1 and 47 μm was measured with a FSSP-100A forward scattering spectrometer probe (Particle Measurement Technology),
- Aerosol particle number concentration and size distribution between 7 and 500 nm was measured with a differential mobility particle sizer,
- Aerosol particle number concentration and size distribution between 0.4 and 19.8 μm was measured with an aerodynamic particle sizer (TSI),
- Surface ozone was measured with a Environnement s/a ozone analyser based on UV absorption,
- External radiation, consisting mainly of cosmic radiation, was measured with a NaI(Tl) scintillation gamma spctrometer,
- High-volume aerosol samples were collected onto glass fibre filters, which were analysed for beryllium-7 using semiconductor gamma spectrometry and lead-210 using alpha counting of the in-grown polonium-210,
- PM10 particle samples were collected onto teflon filters, which were wet digested and analysed for trace metals using ion-coupled plasma mass spectrometry (ICP-MS),

- PM10 particle samples were collected onto teflon filters, which were soxhlet extracted and analysed for polycyclic aromatic hydrocarbons (PAH compounds, e.g. benzo(a)pyrene) using a gas chromatograph with a mass detector, and
- Air samples were collected with steel canisters. The samples were analysed for volatile organic compounds, e.g. propane and butane, using using a gas chromatograph with a flame ionisation detector.

The University of Kuopio measurement programme consisted of ultrafine particles organic fraction atmospheric measurements using an Ultra Fine Organic Tandem Differential Mobility Analyzer (UFO-TDMA). In addition, the Finnish expedition participants participated in several joint measurement programmes:

- MISU performed a meteorological sounding programme with a PTU sounding every sixth hour (00, 06, 12, and 18 UTC). A total of 145 sondes were successfully released,
- Radon-222 was measured using a U.S. Department of Homeland Security, Environmental Measurements Laboratory, instrument based on the in-growth and subsequent alpha counting of short-lived ^{222}Rn progeny,
- MISU's staff collected PM1 samples for the gravimetric determination of mass and ion chromatographic determination of main ions, e.g. sulphate, in the FMI's laboratory,
- UVB radiation was measured with a measurement system of the MISU's single channel sensor and a data logging system of the FMI and the University of Miami, USA,
- Gas bubbles in sea water were measured during the ice drift with an FMI's optical camera system operated by the University of Leeds, UK.
- Additionally, artificial bubble burst sea water particles were measured with the FMI's DMPS and the Uku's UFO-TDMA. The bubble bursting device was mainly operated by the Queensland University of Technology, Australia,
- Cooperation was done in atmospheric particles 3-dimensional concentration measurements during several helicopter flights, the main part of flight measurements were operated operated by a collaboration between MISU and the University of Lund, Sweden, and
- Cooperation was also done in several temperature and aerosol concentration gradient measurements on the arctic pack ice and open leads, the measurements were mainly organized by Leibniz Institute for Tropospheric Research, Germany.

3.2 Instrumentation

High-volume aerosol samples were collected onto glass fibre filters (Munktell MGA), which were analysed for lead-210 using alpha counting of the in-grown polonium-210. The exposed filters and the field blanks were assayed for lead-210 six months after the sampling with an automatic alpha/beta analyser. The technical details of the instrument are described in the report of *Mattsson et al*. (1996). The detector

arrangement consists of five gas-flow proportional counters. The flow gas is P-10, a mixture of argon (90 %) and methane (10 %). The effective window area is 625 cm^2. The counter immediately above the filter has a thin plastic window and is measuring alpha particles. The alpha counting efficiency is 41.5 per cent. The other four counters are for beta particle counting and for anti-coincidence background supression.

For measuring the trace metal concentrations in the air daily PM10 aerosol particle samples were collected with a flow rate of 38.5 l/min on Teflon filters (PTFE, Millipore, 3 µm pore size) during 3 August – 7 September 2008. Trace elements (Al, As, Cd, Co, Cu, Pb, Mn, Ni, Fe, Zn and V) were measured from the samples with an ion-coupled plasma mass spectrometer (Perkin Elmer Sciex Elan 6000) after the digestion with a solution of HF and HNO_3 in an ultrasonic bath.

For measuring the PAH compound concentrations in the air daily PM10 aerosol particle samples were collected with a flow rate of 38.5 l/min on Teflon filters (PTFE, Millipore, 3 µm pore size) according to the standard method EN 12341:1998. Before the analysis in the FMI' laboratory the filters were stored in a freezer. PAH-compounds analyzed in this study were phenantrene, anthracene, fluoranthene, pyrene, benz(a)anthracene, chrycene and triphenylene in the same chromatographic peak, benzo(k)fluoranthene, benzo(b)fluoranthene and benzo(j)fluoranthene in the same chromatographic peak (benzo(k,b,j)fluoranthene), benzo(a)pyrene, benzo(ghi)perylene, indeno(1,2,3-cd)pyrene and dibenz(a,h+a,c)anthracene. Molecule masses of those compounds varies from 178 (phenantrene) to 278 g/mol (dibenzo(a,h+a,c)anthracene). Samples from filters were first extracted 16 hours in dichloromethane using Soxhlet extractor, then dried with sodium sulphate and concentrated to 0.8–1.0 ml volume with rotary evaporator (Büchi) and in thermoblock under nitrogen flow. Deuterated PAH-compounds (phenantrene-d12, chrysene-d12, perylene-d12 and dibenzo(a,h)anthracene-d14, Dr Ehrenstorfer) were used as internal standards and were added into extraction solvent before extraction. External standards with five different concentration levels were used for quantification. The analysis were made using Agilent 6890N gas chromatograph using DB-5ms -column (50m x 0.25mm I.D., film thickness 0.25 µm), and Agilent 5973 mass spectrometric detector for identification and quantification of analyzed compounds.

Particle number size distributions between 7 and 500 nm diameter were measured with a Differential Mobility Particle Sizer (DMPS) system. The DMPS consisted of a Hauke-type Differential Mobility Analyser (DMA) of length 28.5 cm followed by a TSI 3772 Condensation Particle Counter (CPC). The 50% cut-off size of the CPC was 7 nm thus determining the lowest detection limit of the system. The DMPS was operated in closed-loop sheath flow arrangement (*Jokinen and Mäkelä*, 1996) with a flow rate of 11.2 l/min. The inlet and the sample flow rates were both 1 l/min. Time resolution of the system was 6 min. Larger particle size distribution was measured with a TSI Aerosodynamic Particle Sizer (APS). The APS measured in the diameter size range 0.4–19.8 µm in 52 logarithmically divided channels. The time resolution was 5 min.

The Ultra-Fine Organic Tandem Differential Mobility Analyzer (UFO-TDMA) was used during expedition for the detection of an organic fraction in ultrafine 6-60 nm

particles. The working principle of the UFO-TDMA (*Joutsensaari et al*., 2001; *Vaattovaara et al*., 2005) is the following: The UFO-TDMA method utilizes two Differential Mobility Analyzers (DMAs) in series. The first DMA selects a monodisperse sample from a polydisperse aerosol particle population. Then, these particles are brought to a selected subsaturated ethanol vapour environment where they can grow to a new size in accordance their composition and size. This change in size is subsequently monitored with the second DMA. The ratio between the measured size in the second DMA and the size selected in the first DMA is called Ethanol Growth Factor (EGF). During the measurements, the UFO-TDMA selected dry mobility diameters were between 6 and 50 nm.

Aerosol particles were sampled with a minimum interference from the ship and from the sea/ice surface surrounding the ship. The inlet system consisted of two masts (PM10 and PM1) extending at an angle of 45° to about three meters above the laboratory container roof so that the height of the inlet points above sea level was about 25 meters (for more details see *Leck et al*., 2001). The DMPS, the APS and the UFO-TDMA measured most of the time in the same inlet (PM10) where the pre-impactor cuts out particles larger than 10 μm. The DMSP was also occasionally connected to the PM1 inlet line, used in the bubble bursting experiments, and used regularly in the calibrations of Cloud Condensation Nucleus (CCN) counters and an aerosol mass spectrometer (AMS).

The radiosounding program provided a backbone to many of the other observations and radiosondes were released every six hours to measure temperature, humidity and wind speed profiles through the whole troposphere and into the lower stratosphere. Vaisala RS92-SGP digital radiosondes, 350 g Totex rubber balloons filled with helium and the FMI's DigiCORA III sounding processor were used in these measurements. The results are important data for the ground truth and calibration for many of the remote sensing instruments, but they also provide information on the vertical structure of the Arctic atmosphere, in an area where very little such information is available from the regular observation networks.

The ASCOS expedition provided unique *in situ* observations of tropospheric and stratospheric ozone concentration close to the geographical North Pole. The observations were made by balloon borne electrochemical cell type of ozonesondes attached to RS92-SGP radiosondes which were lifted up to the altitude of approximately 35 km by 1200 g Totex balloons. The sounding system was the Vaisala DigiCORA III. The Science Pump Corporation ozonesondes were interfaced to the radiosondes by OIF92 interface. This system allows *in situ* measurements of pressure, temperature, humidity and geolocation together with ozone concentration measurements with a high vertical resolution. In our case the data was obtained with 2 second temporal resolution, which corresponds to a vertical resolution of approximately 10 meters.

The irradiance and surface albedo were measured 3–30 August 2008 at 1-minute resolution at wavelengths of ultraviolet (UV) and photosynthetically active radiation (PAR). For the purpose, a NILU-UV multibandfilterradiometer (MBFR) from NILU Products AS (http://www.nilu.no) was used. The NILU-UV #102 instrument has five

channels (FWHM 10 nm), with nominal center wavelengths at 305, 313, 320, 340, 380 nm, and an additional PAR channel (400–700 nm). The UVB, UV index (*WHO*, 2002), UVA and erythemally weighted (*McKinlay and Diffey*, 1987) UV radiation, total ozone column, and information on cloudiness can be calculated from the measurements as described in *Dahlback* (1996), but radiation measurements alone are not sufficient for further analysis on cloudiness conditions. The radiometer has a Teflon diffuser, silicon detectors, high-quality bandpass filters and is temperature-stabilized to 40°C. One-minute averages of measured irradiances and detector temperature are recorded. The instrument is well maintained and calibrated, and has also participated in the first international intercomparison of MBFRs, arranged in Oslo in 2005 (*Johnsen et al*., 2008).

First the instrument was located on the roof of the meteorological container on the 7th deck above the bridge of icebreaker Oden to measure solar irradiance. During the last four days the instrument was deployed on the ice floe, where it was turned both up- and downwards to achieve albedo data. The periods with a downward-facing sensor varied from one hour (29.8. 13 – 14 UTC) to several (30.8. 16.00 – 24.00 UTC) or 24 hours (27.8. 13 UTC – 28.8. 13.30 UTC). Earlier, *Wüttke et al*. (2006), e.g., have measured Antarctic snow albedo with one sensor (UV-Biometer Model 501 from Solar Light Co. SL501). They measured 1-minute data and rotated the sensor every 10 min. Then, an 8-min mean value of erythemal irradiance was calculated in order to determine the albedo. They neglected the first and last recorded values to be sure that the act of turning the rod is not affecting the calculated albedo. Similarily, we calculated Arctic snow albedo values from our instrument's up/down rotation data (rotation times 27.8. 13 UTC, 28.8. 13.30 UTC, 29.8. 13 UTC, 29.8. 14 UTC, and 30.8. 16 UTC). By using only the data close to the rotation, we can minimize the effect of possible changes in the cloud cover and optical thickness between the periods of upward and downward facing sensor. The turning, fixing and leveling our sensor took maximum of seven minutes which data were neglected. A 3-min mean value of downwelling and reflected irradiances at each measurement channel was calculated in order to determine the albedo. We also calculated the SZA for all these albedo cases, as the Antarctic snow albedo has been reported to change as a function of SZA (*Pirazzini,* 2004).

4. Results and discussion

4.1 Airborne lead-210

Lead-210 (^{210}Pb) is formed in the atmosphere from the radioactive noble gas radon-222 (^{222}Rn) emanating from the Earth's crust. 99 % of the airborne ^{222}Rn originates from land and only 1 % from the sea (*Baskaran et al*., 1993). In the air, ^{222}Rn, being a noble gas, appears as single atoms. Its progeny, including lead-210, are, however, heavy metal atoms and are attached to ambient aerosol particles, the attachment rate depending on the aerosol particle concentration (*Bigg*, 1996). Most of the airborne ^{210}Pb activity is attached to accumulation mode aerosol particles with an

aerodynamic diameter of a few hundred nanometres (*Papastefanou and Bondietti*, 1991; *Sanak et al*., 1981; *Suzuki et al*., 1991; *Suzuki et al*., 1996). Owing to its long half-life (22 years), ^{210}Pb is removed from the atmosphere by different scavenging processes, especially wet deposition, of aerosol particles carrying it rather than by its radioactive decay. Anthropogenic activities do not influence the amount of ^{210}Pb in the air (*Hötzl and Winkler*, 1987). The practically exclusive formation mechanism of airborne ^{210}Pb facilitates its use as a tracer for air masses with a recent contact to land areas (*Preiss et al*. 1996).

The observed ^{210}Pb activity concentrations varied between <5 and 105 μBq/m^3 with a mean value of 32.7 μBq/m^3 (Fig. 2). The value is similar to the ^{210}Pb activity concentrations observed at Ny-Ålesund, Spitzbergen. In 2001-2005 the average ^{210}Pb activity concentration there was 33, 42, and 44 μBq/m^3 in July, August and September, respectively. *Samuelsson et al*. (1986) reported an average concentration of 75 μBq/m³ during a Swedish icebreaker expedition in July–September 1980 between the 75th and 83rd latitude north and between Greenland and Frans Josef Land. The values found at Svalbard are very low compared to continental areas but are clearly higher than in Antarctic areas. For example, the average and maximum monthly ^{210}Pb activity concentrations in Belgrad, Yugoslavia were 1200 and 3170 μBq/m³, respectively (*Todorovic*, 2000). At Marambio research station (64º14'S, 56º43'W) close to the Antarctic peninsula the mean annual ^{210}Pb activity concentration was only 4.5 μBq/m³ in 2005 (*Paatero et al*. 2007). During the ice drift from 13 August to 2 September the average ^{210}Pb activity concentration was 34.3 μBq/m³. Based on the air mass back trajectory calculations with the NOAA/HYSPLIT model (*Draxler and Rolph*, 2003; *Rolph*, 2003) the ice drift period was divided to six classes with different air mass origins (Table 1). The lowest ^{210}Pb activity concentrations, 11.3 μBq/m³, were found in air masses coming from the central Arctic Ocean between the North Pole and the Canadian Arctic archipelago. This value represents the base line of the summer-time ^{210}Pb activity concentration in the surface air in the High Arctic.

Table 1. ^{210}Pb activity concentrations in the air in different air mass origin classes during the ice drift of the ASCOS expedition.

Class	Dates	Main air mass origin	avg. ^{210}Pb act. conc. (μBq/m³)
1	15/8, 20/8, 23/8, 25/8, 26/8	Greenland Sea	27.7
2	14/8, 16/8	Barents Sea	18.4
3	17/8, 18/8, 19/8	Kara Sea, Taimyr peninsula	40.1
4	21/8, 22/8, 24/8	Greenland Sea, Greenland	31.6
5	13/8, 2/9	Western Central Arctic Ocean	11.3
6	27/8, 28/8, 29/8, 30/8, 31/8, 1/9	Eastern Central Arctic Ocean	45.9

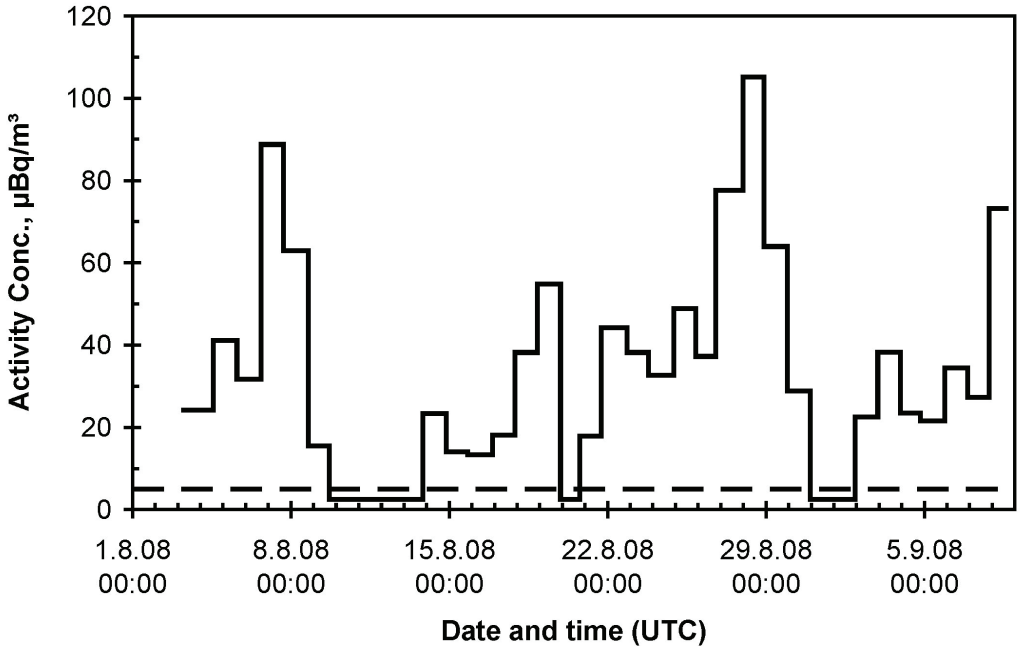

Fig. 2. ^{210}Pb activity concentrations in the air (µBq/m^3) during the ASCOS expedition. The broken line indicates the minimum detectable activity (~5 µBq/m^3).

4.2 Airborne trace metals

The main sources of heavy metals in the Arctic air are natural sources, e.g. sea salt and resuspension of soil particles, and long-range transport from anthropogenic sources in Europe and Russia (*Maenhaut et al*., 1996; *Shevchenko et al*., 2003). In Europe the main sources of heavy metals are combustion of coal and oil in industrial, residential, and commercial boilers, iron, steel and non-ferrous metal production, cement production, waste incineration and road transportation. Nickel originates mainly from petrol refining and public electricity and heat production. Over 40 % of copper and zinc originate from road transport. Metal industry is a significant source as well. The main sources for arsenic are manufacturing industries, constructions and non-ferrous metal industry. According to the UN/ECE/EMEP (United Nations Economic Comission for Europe, European Monitoring and Evaluation Programme) air quality measurements especially the concentrations of Cd and Pb, in air have decreased during the last three decades following closely the trend of emissions. This decrease is mainly caused by the implementation of emission control equipment (*Pacyna et al*., 2009). The mining and metallurgical industry at Norilsk (the largest mining and metal company in Russia) and Kola Peninsula are the most important source of air pollution in Arctic. The nickel, copper and cobalt smelters, apatite mines and iron ore mines emit huge quantities of particles and heavy metals to the atmosphere (*Stebel et al*., 2007).

The trace element levels measured onboard icebreaker Oden were compared to the concentrations measured at the Pallas-Sodankylä Global Atmosphere Watch (GAW)

station in northern Finland. All the cadmium, arsenic and cobalt concentrations measured onboard icebreaker Oden were extremely low, mostly below 0.02 ng/m^3 (Table 2). Furthermore, the concentrations of iron and manganese were lower than those measured at Pallas. During an episode between 10–15 August elevated lead, aluminium and zinc concentrations were observed. At least a part of the time the air masses came from north-western Russia. The concentrations were higher than those detected at the Pallas-Sodankylä GAW station (Fig. 3). The lead concentration level was actually surprisingly high during the whole study period.

Table 2. Statistical summary of the trace metal concentrations in the air (ng/m^3) during the ASCOS expedition. The values below detection limits have been replaced with values of half the detection limits in the calculation of the statistical parameters.

Element	Min. ng/m^3	Max. ng/m^3	Average ng/m^3	Median ng/m^3	Geom. mean ng/m^3
Cd	0.0025	0.0059	0.0027	0.0025	0.0026
Co	0.0025	0.10	0.0076	0.0025	0.0040
Cu	0.065	14.2	1.0	0.25	0.28
Ni	0.14	3.0	0.38	0.20	0.25
Pb	0.029	13.3	0.96	0.27	0.29
V	0.0050	4.97	0.25	0.043	0.051
As	0.010	0.050	0.013	0.010	0.012
Al	0.29	31.1	4.8	2.2	2.2
Fe	1.5	23.2	4.7	4.4	4.0
Mn	0.0080	0.55	0.078	0.041	0.045
Zn	0.040	4.4	0.58	0.22	0.23

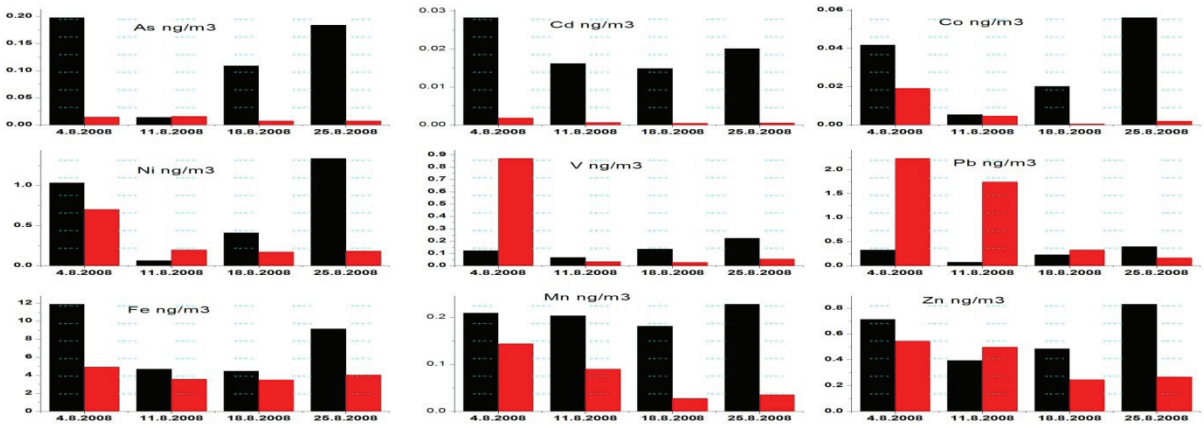

Fig. 3. Trace metal concentrations in the air over the Arctic Ocean (red columns) and at Pallas-Sodankylä GAW station (black columns) in August 2008.

4.3 Airborne PAH compounds

In the atmosphere, the organic fraction of aerosol particles includes a large variety of compounds, which originate from both natural and anthropogenic emissions. Polycyclic aromatic hydrocarbons (PAH compounds) are a particularly harmful part of the organic fraction due to their carcinogenic effect on humans. They are formed during the incomplete burning of organic material and are emitted into the atmosphere from several natural and anthropogenic emission sources. Natural sources include, for example, emissions from forest fires, whereas mainly anthropogenic sources consist of fuel burning in energy and electricity production, traffic and biomass burning (*Ravindra et al*., 2008). Wood combustion, especially in house warming is a great source of PAH compounds, particularly in northern Europe (*Hellen et al*., 2008). Typically, largest PAH concentrations in the air are measured near emission sources, but long-distance transport is also a remarkable source, especially in Northern Europe (*EMEP*, 2008).

First a few selected daily samples were analyzed to obtain information on the overall PAH concentration levels. Those results showed, as expected, that the concentration levels of analysed PAH compounds in the Arctic maritime air are generally very low, in many cases even below detection limits. Because of that, it was decided to combine selected samples together in order to get results above detection limits. Sample combining was made according the simultaneously measured radon-222 activity concentrations. Radon concentrations are useful when differentiating air masses of continental and marine origin. The results show that PAH compound levels in the air on the Arctic Ocean are generally very low, between 0.007–0.24 and 0.0001–0.1 ng/m^3 for total PAH and single components, respectively. A comparison with simultaneous data from Virolahti, southeastern Finland, reveals that PAH concentrations over the central Arctic Ocean were generally 5–20 times lower than at Virolahti.

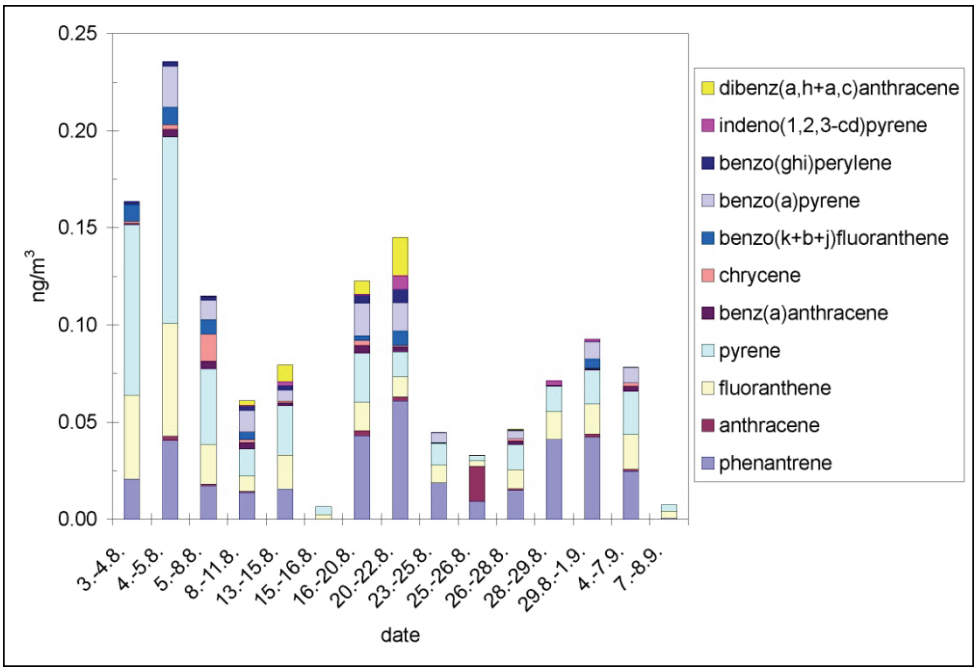

Fig. 4. PAH concentrations in the air over the Arctic Ocean during the ASCOS expedition.

4.4 Aerosol particles

Aerosol particles can have major influence on the Arctic climate change. Particles which act as CCN affect the properties of the clouds, such as their lifetime and scattering characteristics. Particle number and composition affect climate directly by scattering and absorbing the solar and terrestrial radiation. Thus, aerosols are a major factor affecting the warming of the atmosphere. Particle formation has been observed around the world and also in the Arctic (*Leck and Bigg*, 1999; *Kulmala et al*., 2004). However, the source of the particles and their formation mechanisms are still unknown.

In most parts of the world, it is very difficult to study the origin and composition of CCN and their ability to form cloud droplets because there is a great multiplicity of both natural and man-made sources. The Ymer-80 expedition to the fringes of the pack ice region of the central Arctic Ocean (*Lannefors et al*., 1983) was the first major attempt to measure Arctic summer aerosols and trace gases unperturbed from man-made sources. Its results suggested that the central Arctic Ocean in summer might provide a site where there were few sources of aerosols and where optically thin low-level clouds whose reflectivities would be influenced by CCN concentrations were frequent.

Subsequently to the Ymer-80 expedition, *Charlson et al*. (1987) proposed that most of the remote oceanic CCN originated from dimethylsulfide (DMS), a gas released by a temperature-sensitive process in the surface water when zooplankton graze on phytoplankton. These considerations, together with the special importance of the region indicated by climate change models led to its selection for the programs in the summers of 1991, 1996 and 2001.The same motivation was behind ASCOS.

Indeed it was found during IAOE-91 that the oxidation products of gaseous dimethyl sulphide (DMS), such as sulphuric acid, methane sulphonic acid (MSA), and sulphur dioxide (SO2,) were major precursor-components of the CCN-sized particles observed over the pack ice area, although the source of most of the gas was just around the life-affirming ice edges of the pack ice area (*Leck and Persson*, 1996a; *Leck and Persson*, 1996b). This was consistent with the idea that, as the winds carried air rich in DMS towards the Pole, nuclei mode particles (a few nm in diameter) of sulphuric acid were formed. Subsequently, these particles grew slowly to become large enough (accumulation mode ca 100nm diameter) by further condensation of the acids to act as cores for activation into cloud droplets. However, as fogs and low cloud were found to cause a very rapid turnover of particles entering the atmosphere over the pack ice (*Nilsson and Leck*, 2002) it seemed relevant to ask the question: How could the particles survive long enough in the presence of frequent fogs and low-level clouds to grow sufficiently to become CCN? It had to be assumed that formation and growth were in the free troposphere above the boundary layer, and that they were later mixed down to the surface (*Wiedensohler et al*., 1996). This assumption would also have to explain the appearance of Aitken mode particles (25–70nm diameter) at the same time.

The next expedition (AOE-96) to the same area aimed to study the aerosol evolution in more detail. There were more nucleation events than in 1991 and they were found in air that had its last contact with the surrounding seas, more that four days ago.

Again the nucleation mode particles were usually accompanied by particles in the Aitken mode. To test the idea that they are made of sulphuric acid, they were examined by electron microscopy (*Bigg and Leck*, 2001). To a great surprise, these very small particles, when present, were not at all composed of sulphuric acid. Instead, they were mostly five or six-sided insoluble solids, resembling viruses or microcolloids, and were accompanied by larger particles such as aggregated compact balls, bacteria and fragments of diatoms.

A hypothesis (*Leck and Bigg*, 1999) was advanced that assumed that the most likely source for these particles is the open water between ice floes and started with the bursting of air bubbles on the open leads. The bubbles would scavenge soluble proteins, particulate organics and bacterial enzymes from the water. Upon bursting, these were injected into the air from the bubble film or the jet drops that followed its collapse. Once involved in fog or haze drops, the bacterial enzymes would release the amino acid, L-methionine from the proteins. This compound, alone amongst the 20 common amino acids is only found in its oxidised form in the atmosphere and was found in the laboratory to lead to nucleation of new particles. Because the solid Aitken particles were associated with the nucleation events it was further suggested that the evaporation of haze or fog drops led to both the nucleation and co-production of particles up to ca 50nm in diameter.

Some of the unfinished business from AOE-96 therefore was to test the nucleation hypothesis, to establish the source of the Aitken particles and to improve our knowledge of the influence of meteorological conditions upon production and evolution of all particles. In addition to extending the meteorological, chemical and physical measurements made during AOE-96 a wide-ranging biological program in water and ice was necessary to characterize potential sources of particulates and soluble organic compounds of the leads.

Vertical profiling of particles during AOE-2001 showed that the formation of the nuclei mode particles around 10nm diameter indeed was taking place in the shallow boundary layer (ca 200m deep) below the capping inversion in regions recently occupied by cloud or fog the clouds. The assumptions made in by *Leck and Bigg* (1999) were consistent with the observations but it has not been possible to identify positively the amino acid L-Methionine as the nucleating agent.

The vertical profiling also verified earlier observations that the nucleation mode particles were accompanied by particles in the Aitken mode. To search for evidence of a fog-related aerosol source in the high Arctic summer the aerosol size distribution data taken during AOE-96, and AOE-2001 were combined (*Heintzenberg et al*., 2006). On average the Aitken mode concentrations increased strongly above their respective fog-period-medians in both years before maximum drop numbers were reached during the fog. The results were interpreted as a strong indication of fog-related aerosol source processes as discussed in *Leck and Bigg* in 1999. This needs to be elucidated with further data from dedicated fog experiments in future Arctic expeditions in order to understand the life cycle of the aerosol north of 80°.

To examine the particulate material within the surface microlayer (<100μm thick surface film of the open water between the ice flows) a radio-controlled miniature boat was used. Particles in this surface microlayer were extremely numerous, ranging between 106 and 1014 ml-1 (*Bigg et al*., 2004). They were often aggregated into compact balls <100nm in diameter, closely resembling microcolloids or "virus-like particles". Particles were simultaneously collected from the atmosphere. The morphologies, chemical and physical properties of airborne particles were closely similar to those of the microlayer particulates (*Leck and Bigg*, 2005a). This strongly suggested that the airborne particles were ejected from the water by bursting bubbles. Accompanying the particles in both air and water was a gel-like substance, the properties of which identified it as having been formed from the exopolymer secretions (EPS) of the resident ice algae and bacteria. EPS gels consist of large, highly surface-active highly hydrated (99% water) molecules (*Decho*, 1990). They are polysaccharides to which other organic compounds such as proteins, peptides and amino acids are readily bound. The gels collapse under the influence of ultraviolet light or acidification (*Chin et al*., 1998; *Orellana and Verdugo*, 2003). Their lifetime in the atmosphere is therefore limited and the collapse of the structure with such strong water retentive properties explains some of the puzzling features of the aerosols observed over the pack ice. For example the expulsion of water as the gel collapses may explain why airborne aggregates and bacteria very rarely have attached sea salt (*Bigg and Leck*, 2008). The breakup of aggregates when the joining EPS gel collapses is a process that would be governed by repeated condensation and dissipation of fogs or clouds in accordance with the strong indication of fog-related aerosol source mention above. It is also a sufficient reason why the airborne aggregate size distribution so closely resembles that of the surface microlayer aggregates but is shifted to a smaller modal diameter (30nm instead of 50nm). On average, during the five weeks spent in the pack ice region during 2001, surface microlayer-derived particles represented more than one-half of the collected airborne submicrometre particle and more than four-fifths on sunny days when melting of the fringes of the ice floes was observed. On all days surface microlayer-derived particles dominated the population below 70 nm diameter, the Aitken mode.

Fresh aggregates with EPS gel on them could act as CCN directly because of the gel's strong surface-active properties. Those that have lost their gel could still act as sites for condensation of the oxidation products of DMS. Evidence that this happens is the detection of insoluble marine microcolloids in most (50–90% of total number counted, *Leck and Bigg*, 2005b) of the predominantly sulphate particles. Their acquisition of sulphuric acid provides a much more direct and faster path to CCN status than having to grow from nucleated particles. Moreover, a recent model study by *Lohmann and Leck* (2005) found it necessary to invoke a highly surface-active Aitken mode, assumed to be EPS, externally mixed with a sulphur-containing population in order to explain the observed CCN over the pack ice. This gives extra weight to the importance of the surface microlayer in forming the clouds of the high Arctic.

With this new picture of the evolution of the remote Arctic aerosol, DMS concentration will determine the mass of sulphate produced by producing material for

growth of the particles but will have only a minor influence on the number of CCN and thus cloud droplets. That will be mainly dictated by the number of airborne microcolloids.

A fraction of the particles might grow to sizes where they can activate as cloud droplets. Critical questions to resolve in the Arctic are: How, when and where new particles form, are these particles able to grow to CCN sizes and which particles are most likely to activate as CCN? Our results aim to get closer to the answers of the questions.

The usefulness of the UFO-TDMA in marine conditions has been demonstrated in laboratory measurements for 6–50 nm (in diameter) particles (*Vaattovaara et al*., 2005). It is due to the fact that atmospherically important ultrafine inorganic particles, sodium chloride and the ammonium sulfate, do not grow (i.e. EGF is 1) in the subsaturated (S=82–84%) ethanol vapour. On the other hand, particles composed of biogenic organic compounds (e.g., citric or tartaric acid) do grow (i.e. EGF is clearly over 1) at sizes 8–50 nm. Importantly, these measurements are consistent with the bulk ethanol solubility of inorganic and organic compounds given in the literature (e.g., *CRC Handbook of Chemistry and Physics*, 1996).

Based on the measured EGFs for 8, 10, 15, 20, 30, 40, 50, and 60 nm particles, respectively, an estimate of a minimum organic volume fraction (OVF) can be carried out in the particles. This analysis principle, based on the difference in organic and inorganic particles ethanol solubility (*Vaattovaara et al*. 2005), is similar to OVF analysis introduced in *Vaattovaara et al*. (2006).

During the ASCOS expedition the aerosol particle total number in the clean Arctic air was in minimum below 10 cm^{-3}, actually frequent zero values were detected during the cleanest cases. Such low numbers indicate a lack of local sources in conditions where the long-distance transport is also weak. However, occasionally particle number increased to several 100 cm-3 and these high concentrations were often connected with the appearance of small nucleation and Aitken mode particles. Life time of such small particles is on the order of hours. Thus the gas phase option must be presented as an additional suggestion.

A more detailed study was performed on an event detected in the late evening of 20 August 2008 (Fig. 5). Air mass back trajectories were calculated with the NOAA/HYSPLIT (Hybrid Single Particle Lagrangian Integrated Trajectory Model, *Draxler and Rolph*, 2003; *Rolph*, 2003) model every three hours for the heights of 50, 500 and 1000 m. The air masses arriving at 50 m level came from the west coast of Greenland descending at the coast line during both 20 and 21 August. Higher level air masses arrived on 20 August from the east over the central Arctic Ocean then turning to west on 21 and following the route of the 50 m trajectories. As no major differences were detected in the lowest level air masses, the changes seen on particle numbers and distributions were assumed to be mostly related to local natural sources and weather phenomena rather than air mass origin. The local weather at the time of the nucleation mode appearance was cloudy.

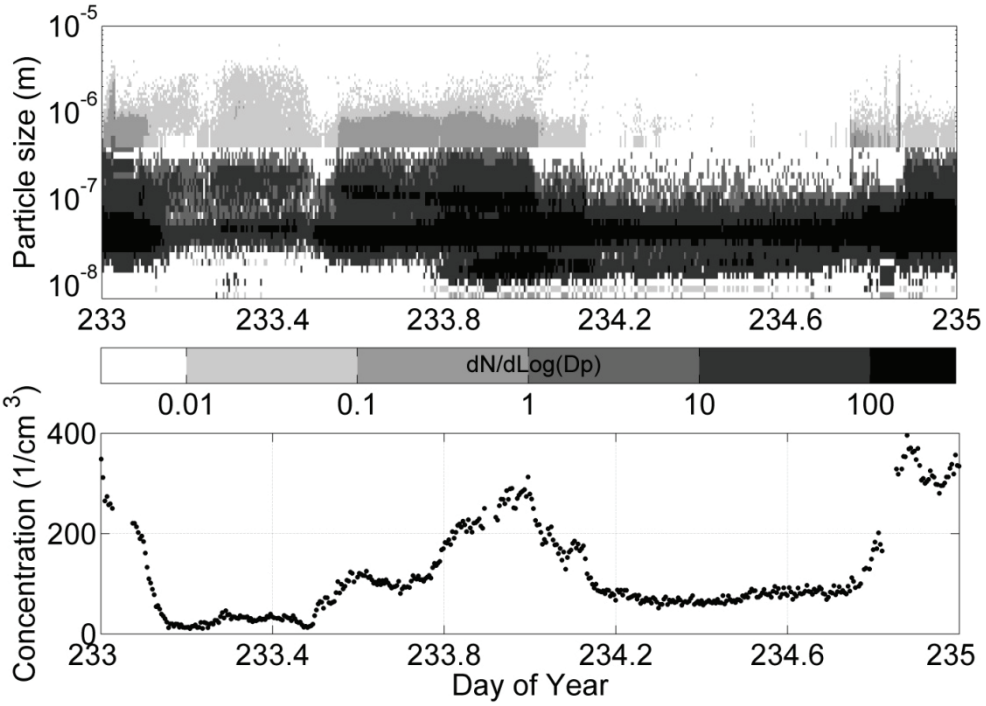

Fig. 5. Aerosol particle number size distribution between 7 nm and 10 μm diameter (upper panel) and total particle number (lower panel) measured on 20–21 August 2008.

At around midday on UTC time on 20 August an increase was detected in both the Aitken and accumulation mode concentrations. Later in the evening (at 19 pm UTC, ship location 87.407 N°; 7.646 W°) also a growing nucleation mode was detected. Formation and growth of the particles depends on both the amount of the condensing vapours (source) and the background particle distribution (sink). At the time of the appearance of the nucleation mode the background concentrations were relatively high, thus probably decreasing the nucleation mode particle number. The growth rate of the particles was calculated by fitting lognormal modes to the growing nucleation mode and making a linear fit to the mode median diameters. This method gave a growth rate of 0.7 nm/h. If we further assume a constant growth rate of the 10 nm particles in diameter, their formation time at 1 nm was the early morning of the 20 August. At 6 am the 50 m trajectory was close to the ground over the pack-ice and travelled about one day ahead from the coast of the Greenland. As the coast of the Greenland is partly unfrozen at the summertime, it is a possible origin of the nucleating and condensing vapours such as organics, in addition to open leads over the pack ice region.

Based on the UFO-TDMA measurements estimated minimum organic volume fractions (OVF) were 55–65% for 15 nm particles before midnight when nucleation mode size particles were present. At the same time, the estimated OVF of 50 nm particles was about 60–70%. This supports the assumption that the organics seem to play a key role in the particle growth during the evening of 20 August.

Particle numbers in the Arctic are low but increase occasionally due to e.g. small freshly nucleated particles (*Lannefors et al*., 1983; *Covert et al*., 1996; *Bigg et al*., 1996). The small nucleation and Aitken mode particles contain a large fraction of

organics which then seem to be the main components responsible for the particle growth. The results will help to understand the complex Arctic climate system. In the near future the aim is to connect the whole instrumentation on board ship Oden to provide additional insights into the data.

4.5 Meteorology soundings

Figure 6 provides examples of some of the meteorological sounding data and illustrates the characteristics of the Arctic summer atmosphere. Figure 6a and b show the probability of equivalent potential temperature, Θ_e, and relative humidity, RH, respectively. Additionally the mean (solid) and median (dashed) profiles are included in each panel. A brief inspection of these plots reveals a layer close to the surface with predominantly constant Θ_e and (high) RH with height. Interestingly, while this layer is on average some 500 meters deep in temperature, the very moist (RH ~ 100%) layer is deeper, reaching up to about a kilometer. This suggests that in contrast to continental well mixed boundary layers, the high moisture in the Arctic boundary layer, and thus the potential for clouds, reaches well into the inversion layer.

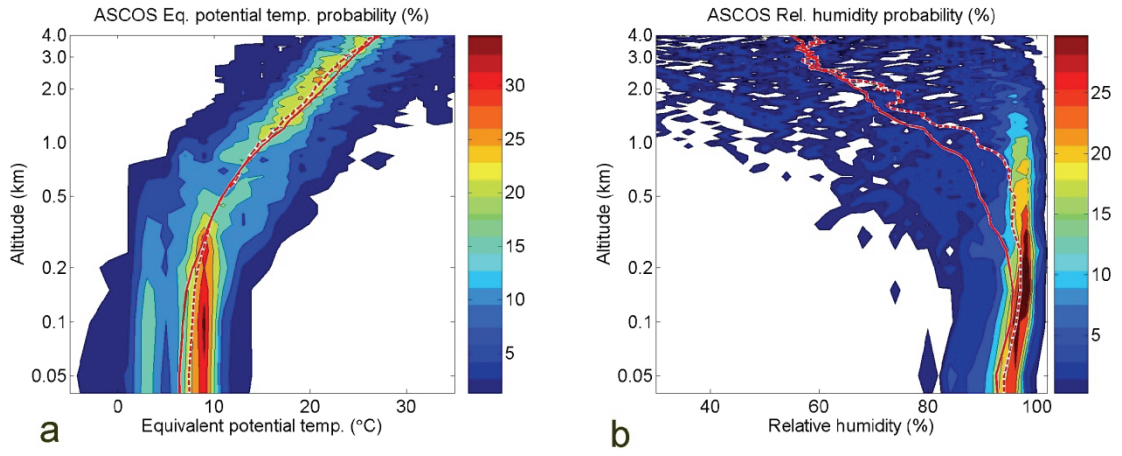

Fig. 6. Plots of probability as a function of height of (a) equivalent potential temperature and (b) relative humidity. The plots are based on all 145 soundings during ASCOS.

In Figure 7, the probability of the vertical gradient of Θ_e corresponding to Figure 6a is shown. It is again clear that the gradient of Θ_e is constant and close to zero (near-neutral stratification) in the lowest few hundred meters; interestingly there is a shallow layer between approximately 300 and 500 meters where the peak of the PDF of gradient is actually at zero. As this is a layer most often occupied by low clouds this indicates that there is a potential for shallow convection in this layer. The largest values of the Θ_e-gradient are typically found in a layer between approximately 400 meters and 1 kilometer. This is indicative for the persistent inversion, capping the boundary layer.

The prevailing wind speed profile (Figure 8) shows a weak low-level maximum between about 200 and 800 meters, indicative of the presence of a low level jet. This jet was stronger on occasions and absent on others; the fact that it shows up in the PDF however, suggest it was fairly common.

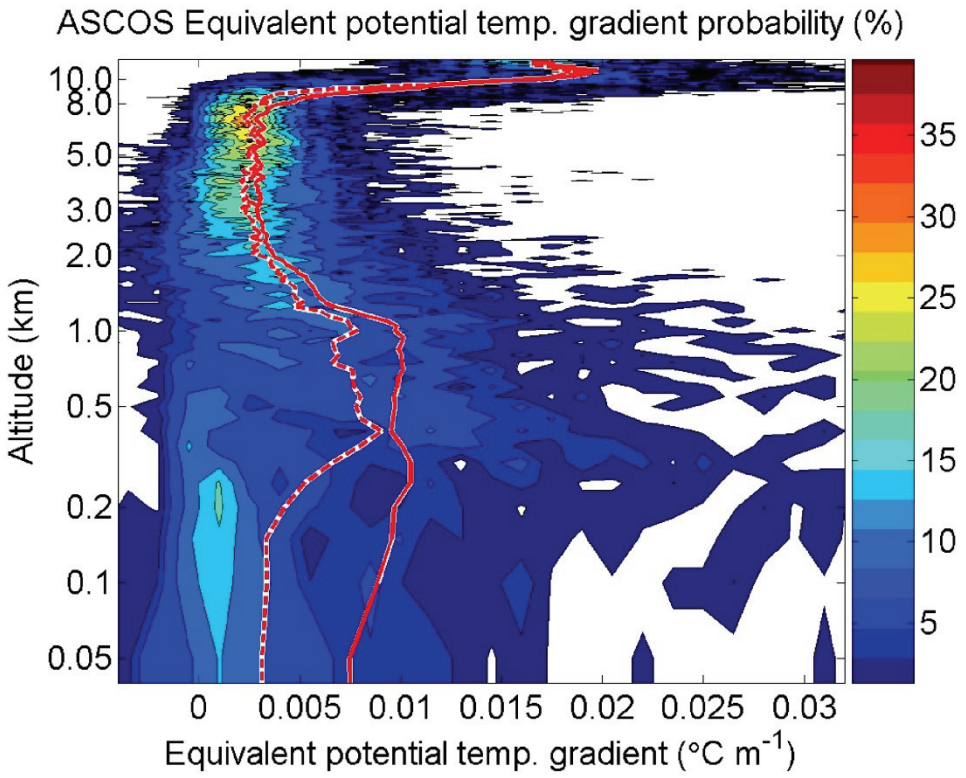

Fig. 7. Same as Fig. 6, but for the vertical gradient of the equivalent potential temperature.

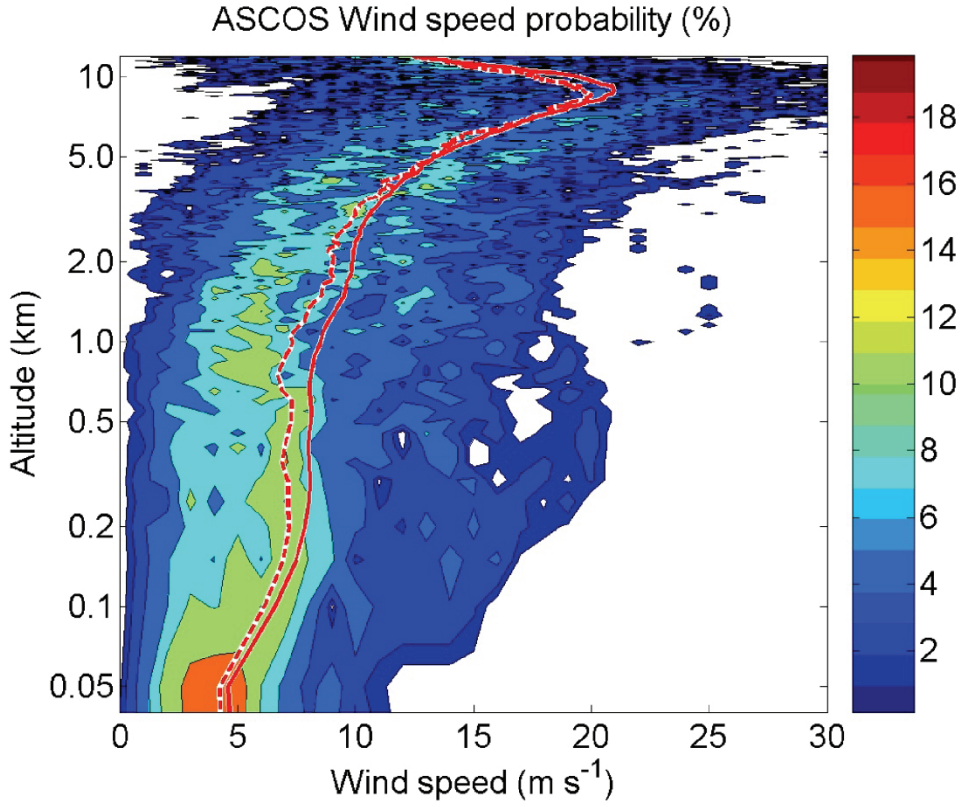

Fig. 8. Same as Fig. 6, but for the vertical profiles of wind speed.

4.6 Ozone soundings

The seasonal cycle of stratospheric ozone over the northern high latitudes shows maximum in late winter/spring and minimum late summer or early autumn (*Kivi et al*., 2007). The minimum ozone abundance in late summer is the result of weakening of the Brewer-Dobson mean meridional circulation in summer and secondly the catalytic gas-phase chemical reactions, which are dominated by nitrogen and hydrogen cycles. It turns out that under constant insolation in summer the catalytic cycles involving NO_x are able to destroy more ozone than is photochemically produced locally or transported from lower latitudes. Therefore ozone column is constantly reduced during the Arctic summer and results in a pool of low column ozone over the polar area in summer (*Fahey and Ravishankara*, 1999). In shorter time scales fluctuations of stratospheric and thus total ozone are caused by atmospheric motions through vertical and horizontal transport. Synoptic weather systems are known to cause variations in column ozone. However, synoptic variability is relatively weak in summer compared to other seasons. The same applies for the inter-annual variability, which is the lowest in summer at northern high latitudes (*Kivi et al*., 2007).

The ozone measurements reported here were obtained far from the sites of regular observations, in the vicinity of the North Pole. Alert in Northern Canada (located at 82.5°N, 62.3°W) is currently the northernmost station providing such measurements of high vertical resolution. Ny-Ålesund (located at 78.9°N, 11.9°E) was geographically the closest permanent sonde station during the campaign. The sounding times along with the geographic location are shown in Table 3. The first five soundings were made during the ice drift period 22-31 August 2008 (Fig. 9). The main features are that the altitude region from 25 to 35 km shows little day-to-day variations, while dynamically induced variability is large in the altitude region of roughly 20–25 km and 6–12 km. The variability at the lower layer can be explained by variations in tropopause altitude. During the ozonesonde measurements the tropopause altitude varied between 6 and 10 km of altitude (Fig. 10) and the variations were significant during the first days of the ozone soundings, with descending tropopause during the second launch and ascending afterwards. The column ozone changed according to the tropopause movements (Table 3). There is a remarkable layer of ozone-poor air at about 13 km of altitude, which shows little amount of day-to-day variations. It turns out that this layer corresponds to climatological minimum, which shows up at all high-latitude ozone sonde stations and is most pronounced in summer (*Kivi et al*., 2007). The origin of the layer of low ozone is not completely understood, it has been suggested that it may be related to the quasi-isentropic advection of ozone-poor air from lower latitudes. Variations in the tropospheric ozone concentration may be related to long-range transport from distant source regions.

Table 3. Ozone sonde launch times and coordinates, estimates of the total column ozone based on the ozone sonde data and corresponding tropopause pressure values.

Date	Time (UTC)	Lat. °N	Long. °E	Total ozone (DU)	Tropopause pressure (hPa)
22-Aug-08	18	87.37	-7.47	300	291.4
25-Aug-08	12	87.42	-7.42	311	345.1
27-Aug-08	11	87.35	-8.52	287	257.0
29-Aug-08	12	87.25	-9.53	292	262.8
31-Aug-08	12	87.18	-9.79	264	254.9
02-Sep-08	12	86.86	-1.53	-	245.2
04-Sep-08	17	84.16	0.39	296	310.0
06-Sep-08	11	80.68	9.36	297	258.1

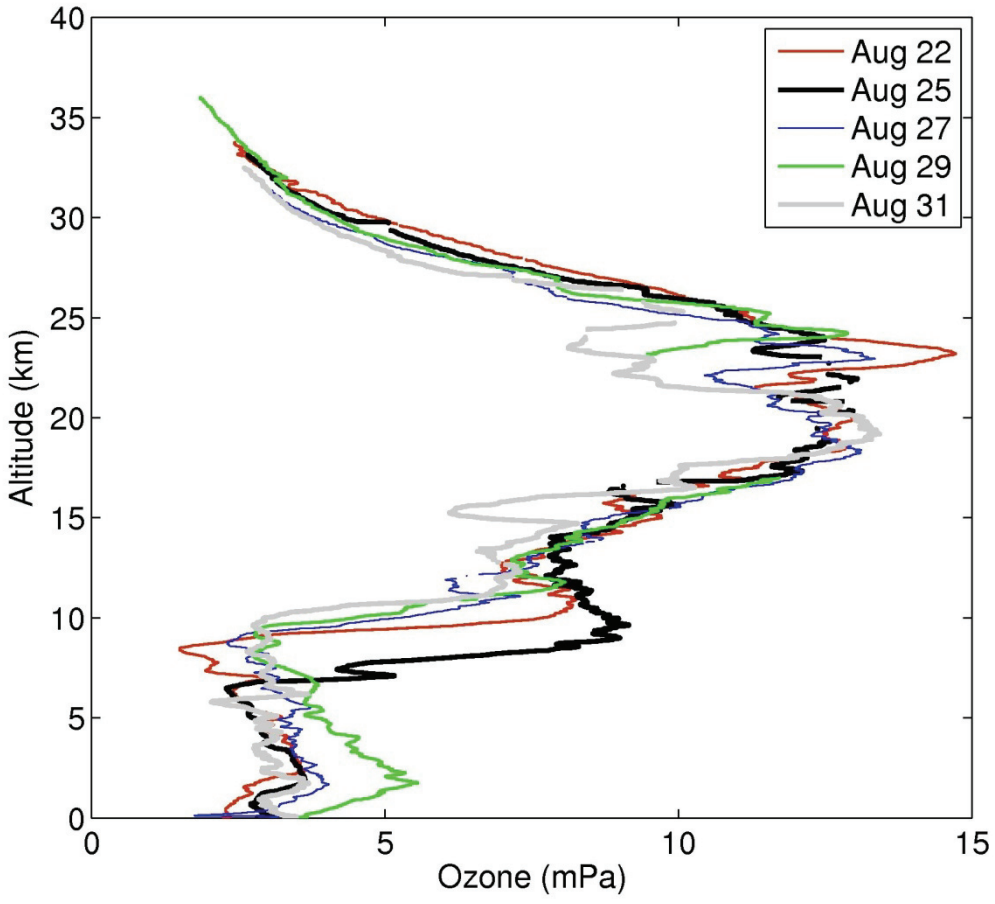

Fig. 9. Ozone partial pressure profiles obtained during the time period 22–31 August at approximately 87°N.

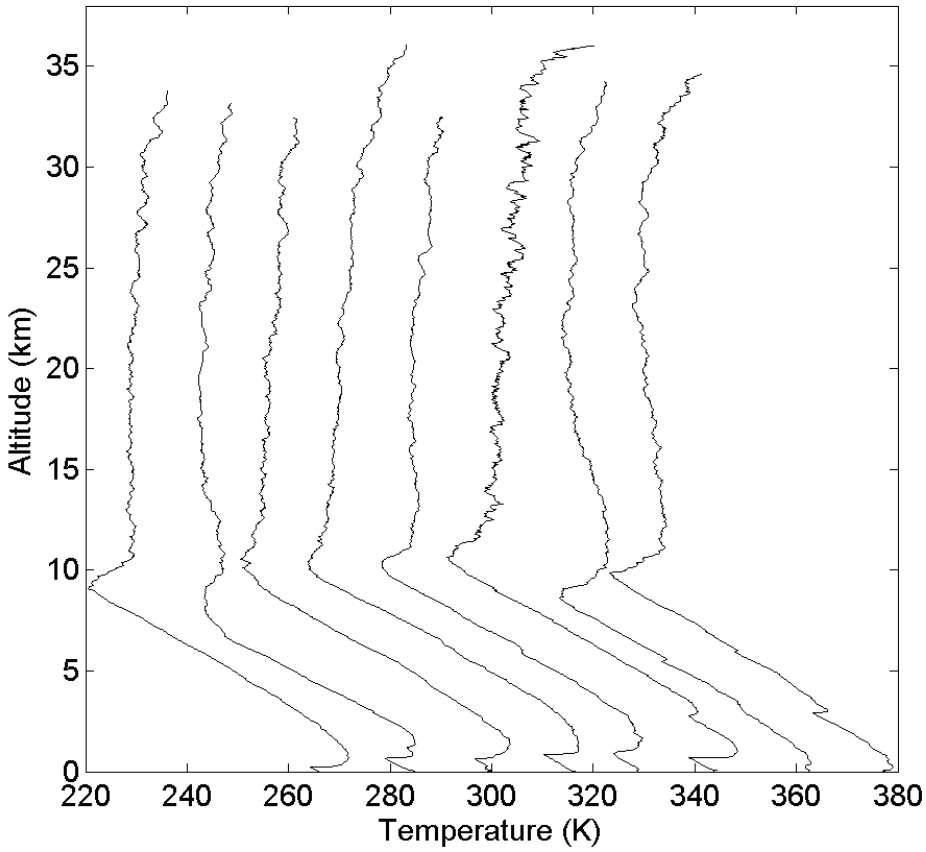

Fig. 10. Temperature profiles obtained during the ozone soundings. The launch dates are from left to right: August 22, 25, 27, 29, 31; September 2, 4, 6, 2008. The first profile represents absolute values the next ones are shifted by adding 15 K to the previous profile.

4.7 Ultraviolet and photosynthetically active radiation

The average of the 3-min mean values of snow UV and PAR albedo was 0.92 (Table 4). At the low wavelengths of the channel 1 (305 nm), the measured intensities were very low and the determination of albedo more uncertain. We also calculated the 8-min means for albedo, and found changes in cloudiness to increase the uncertainty albedo calculation at PAR. UV results remained unaffected. The 8-min mean values were found to differ by less than 0.01 from the 3-min values for most of the cases. All the measurements represented a similar SZA (~ 77–79 deg). Thus, the possible SZA dependency cannot be studied. The latitude for our albedo measurements was very high, 87 ^{o}N. *Grennfell et al*. (1994), have reported the exceptionally clean snow albedo at the South Pole (90 ^{o}S) to be 0.98 and uniform across the spectrum. *Perovich* (2002), in turn, reported albedo of 0.9 over shore-fast sea ice at Barrow Alaska (71 ^{o}N) and explained the difference to result from the large amount of particulates present in the Barrow snow pack compared to the Grennfell's results from South Pole. On the basis of the ASCOS results, the low amount of particles is not expected to have an influence on our surface albedo values. The use of one sensor eliminates the effect of different cosine errors, and

ensures the same spectral and radiometric responsitivity, and we consider our 3-min mean albedo values of A = 0.91–0.92 for UV and PAR, a representative sample of Arctic Sea ice and snow albedo at 87 ^{o}N in August 2009. Compared to the Surface SHEBA-field experiment on Heat Budget of the Arctic Ocean at 70–80 ^{o}N (http://www.eol.ucar.edu/projects/sheba/), our albedo values are equal to those (A > 0.9) reported for the Arctic Sea in April for 400 nm and 600 nm by Perovich et al. (2002, Fig. 11). In August, due to snow melt, their albedos were ~ 0.7. Earlier, we have measured Arctic snow albedo at 67 °N in the Finnish Lappland, and found the midday erythemally weighted UV albedo ranging from 0.6 to 0.8 in the accumulation period and 0.5–0.7 during melting (*Meinander et al*., 2008). The temporal and spatial variability of Arctic snow/ice albedo appears therefore significant, and requires ancillary environmental information, e.g., on the amount of particles or the snow grain size, in order to be understood.

Table 4. Albedo of snow at 305, 313, 320, 340, 380 nm, and of PAR (400–700 nm), calculated from the raw values of one radiometer turned up and down.

Date Time, UTC	**LAT**	**LON**	**SZA**	**305**	**313**	**320**	**340**	**380**	**PAR**
27.8. 13	87.352	-8.638	76.97	0.94	0.92	0.92	0.92	0.92	0.92
28.8. 13.30	87.295	-9.433	77.27	0.92	0.91	0.91	0.91	0.92	0.93
29.8. 13	87.248	-9.475	77.57	0.95	0.92	0.92	0.92	0.92	0.91
29.8. 14	87.247	-9.445	77.73	0.97	0.96	0.95	0.95	0.96	0.92
30.8. 16	87.206	-9.501	78.89	0.97	0.91	0.91	0.91	0.92	0.93

5. Conclusions

The ASCOS expedition brought unique data from the High Arctic as it was the only IPY project dealing with the atmosphere in the area. The Finnish measurement and sampling programme produced data and samples from the ocean surface water up to the upper stratosphere. To the best of our knowledge e.g. radioactivity soundings have never before performed at such high latitudes. The UFO-TDMA measurements were also carried out the first time over the central Arctic Ocean. Only some preliminary results are presented here, as the laboratory analyses of the samples and the detailed analyses of the data is expected to last several years. But already now it has become evident that the data gathered during the expedition will bring new information on e.g. aerosol particle formation mechanisms over the central Arctic Ocean.

Acknowledgements

This work is part of ASCOS (the Arctic Summer Cloud Ocean Study) and was funded by the Finnish Meteorological Institute, the University of Kuopio, the Academy of Finland, Finnish Academy of Science and Letters/Vilho, Yrjö and Kalle Väisälä

Foundation, and the Finnish Cultural Foundation, Lapland Regional fund. ASCOS was made possible by funding from the Knut and Alice Wallenberg Foundation and the DAMOCLES European Union 6th Framework Program Integrated Research Project. The Swedish Polar Research Secretariat (SPRS) provided access to the icebreaker Oden and logistical support. We are grateful to the SPRS logistical staff and to Oden's Captain Mattias Peterson and his crew. ASCOS is an IPY project under the AICIA-IPY umbrella and an endorsed SOLAS project.

References

ACIA, 2004. Impacts of a Warming Arctic: Arctic Climate Impact Assessment. Cambridge: Cambridge University Press.

Baskaran, M., C.H. Coleman and P.H. Santschi, 1993. Atmospheric Depositional Fluxes of ^{7}Be and ^{210}Pb at Galveston and College Station, Texas. *J. Geophys. Res.*, **98**, 20555–20571.

Bigg, E.K., 1996. Ion-induced nucleation around radon daughters in remote Arctic maritime air. *Tellus,* **48B**, 322–328.

Bigg, E.K., C. Leck and E.D. Nilsson, 1996. Sudden changes in arctic atmospheric aerosol concentrations during summer and autumn. *Tellus*, **48B**, 254–271.

Bigg, E.K., and C. Leck, 2001. Properties of the aerosol over the central Arctic Ocean. *J. Geophys. Res.*, **106**, 32101-32109.

Bigg, E. K. and C. Leck, 2008. The composition of fragments of bubble bursting at the ocean surface. *J. Geophys. Res.*, **113**, D11209, doi:10.1029/2007/JD009078.

Bigg, E.K., C. Leck and L. Tranvik, 2004. Particulates of the surface microlayer of open water in the central Arctic Ocean in summer. *Marine Chem.,* **91**, 131–141.

Charlson, R.J., J.E. Lovelock, M.O. Andrea and S.G. Warren, 1987. Oceanic phytoplankton, atmospheric sulfur, cloud albedo and climate. *Nature*, **326,** 655–661.

Chin, W.-C., M.V. Orellana and P. Verdugo, 1998. Spontaneous assembly of marine dissolved organic matter into polymer gels. *Natur*e, **391**, 568–572.

Covert D.S., A. Wiedensohler, P.P. Aalto, J. Heintzenberg, P.H. McMurry and C. Leck, 1996. Aerosol number size distributions from 3 to 500nm diameter in the arctic marine boundary layer during summer and autumn. *Tellus*, **48B**, 197–212.

CRC Handbook of Chemistry and Physics, 1996, 77th Edition, CRC press.

Dahlback, A., 1996. Measurements of biologically effective UV doses, total ozone abundances, and cloud effects with multichannel, moderate bandwidth filter instruments. *Appl. Opt.,* **35**, 6514–6521.

Decho, A.W., 1990. Microbial exopolymer secretions in ocean environments: Their role(s) in food webs and marine processes. *Oceanogr. Mar. Biol. Ann. Rev*., **28**, 73–153.

Draxler, R.R. and G.D. Rolph, 2003. HYSPLIT (Hybrid Single-Particle Lagrangian Integrated Trajectory). Model access via NOAA ARL READY Website (http://www.arl.noaa.gov/ready/hysplit4.html), Silver Spring, MD: NOAA Air Resources Laboratory.

EMEP, 2008. Persistent Organic Pollutants in the Environment. Status Report 3/08. Joint EMEP MSC-E & CCC Report.

Fahey, D.W. and A.R. Ravishankara, 1999. Summer in the stratosphere. *Science,* **285**, 208–210.

Grenfell, T.C., S.G. Warren and P.C. Mullen, 1994. Reflection of solar radiation by the Antarctic snow surface at ultraviolet, visible, and near infrared wavelengths. *J. Geophys. Res.*, **99**, 18669–18684.

Heintzenberg, J., C. Leck, W. Birmili, B. Wehner, M. Tjernström, M. and A. Wiedensohler, 2006. Aerosol number-size distributions during clear and fog periods in the summer high Arctic: 1991, 1996 and 2001. *Tellus*, **58**, 41–50.

Hellen, H., H. Hakola, S. Haaparanta, H. Pietarila and M. Kauhaniemi, 2008. Influence of residential wood combustion on local air quality. *Sci. Tot. Environ.*, **393**, 283–290.

Hötzl, H. and R. Winkler, 1987. Activity Concentrations of ^{226}Ra, ^{228}Ra, ^{210}Pb, ^{40}K and ^{7}Be and their Temporal Variations in Surface Air. *J. Environ. Radioact.*, **5**, 445–458.

Intrieri, J.M., C.W. Fairall, M.D. Shupe, P.O.G. Persson, E.L. Andreas, P.S. Guest and R.E. Moritz, 2002a. An annual cycle of Arctic surface cloud forcing at SHEBA. *J. Geophys. Res.,* **107**, doi:10.1029/2000JC000439.

Intrieri, J.M., M.D. Shupe, T. Uttal, and B.J. McCarty, 2002b. An annual cycle of Arctic cloud characteristics observed by radar and lidar at SHEBA. *J. Geophys. Res.,* **107**, doi:10.1029/2000JC000423.

Johnsen, B., B. Kjeldstad, T.N. Aalerud, L.T. Nilsen, J. Schreder, M. Blumthaler, G. Bernhard, C. Topaloglou, O. Meinander, A. Bagheri, J.R. Slusser, and J. Davis, 2008. Intercomparison and harmonization of UV Index measurements from multiband filter radiometers. *J. Geophys. Res.,* **113**, doi:10.1029/2007JD009731.

Jokinen, V. and J. Mäkelä, 1996. Closed loop arrangement with critical orifice for DMA sheath/excess flow system. *J. Aerosol Sci.*, **28**, 643–648.

Joutsensaari, J., P. Vaattovaara, M. Vesterinen, K. Hämeri and A. Laaksonen, 2001. A novel tandem differential mobility analyzer with organic vapor treatment of aerosol particles. *Atmos. Chem. Phys.* **1**, 51–60.

Kivi, R., E. Kyrö, T. Turunen, N.R.P. Harris, P. von der Gathen, M. Rex, S.B. Andersen and I. Wohltmann, 2007. Ozonesonde observations in the Arctic during 1989–2003: Ozone variability and trends in the lower stratosphere and free troposphere. *J. Geophys. Res.*, **112**, doi:10.1029/2006JD007271.

Kulmala, M., H. Vehkamäki, T. Petäjä, M. Dal Maso, A. Lauri, A., V.-M. Kerminen, W. Birmili and P.H. McMurry, 2004. Formation and growth rates of ultrafine atmospheric particles: A review of observations. *J. Aerosol Sci.*, **35**, 143–176.

Lannefors, H., J. Heintzenberg and H.-C. Hansson, 1983. A comprehensive study of physical and chemical parameters of the Arctic summer aerosol; results from the Swedish expedition Ymer-80. *Tellus,* **35B**, 40–54.

Leck, C. and E.K. Bigg, 1999. Aerosol production over remote marine areas - A new route. *Geophys. Res. Lett.*, **23**, 3577–3581.

Leck, C. and E.K. Bigg, 2005a. Biogenic particles in the surface microlayer and overlaying atmosphere in the central Arctic Ocean during summer. *Tellus,* **57B**, 305–316.

Leck, C. and E.K. Bigg, 2005b. Evolution of the marine aerosol – A new perspective. *Geophys. Res. Lett.,* **32**, doi: 10.1029/2005GL023651.

Leck, C., E.K. Bigg, D.S. Covert, J. Heintzenberg, W. Maenhaut, E.D. Nilsson and A. Wiedensohler, 1996. Overview of the atmospheric research program during the International Arctic Ocean Expedition of 1991 (IAOE-91) and its scientific results. *Tellus*, **48**, 136–155.

Leck, C. and C. Persson, 1996a. The central Arctic Ocean as a source of dimethyl sulfide – Seasonal variability in relation to biological activity. *Tellus*, **48B**, 156–177.

Leck, C. and C. Persson, 1996b. Seasonal and short-term variability in dimethyl sulfide, sulfur dioxide and biogenic sulfur and sea salt aerosol particles in the arctic marine boundary layer, during summer and autumn. *Tellus,* **48B**, 272–299.

Leck, C., E.D. Nilsson, E.K., Bigg and L. Bäcklin, 2001. Atmospheric program on the Arctic Ocean Expedition 1996 (AOE-96): An overview of scientific goals, experimental approach, and instruments. *J. Geophys. Res.,* **106**: 32051–32067.

Leck, C. and E.K. Bigg, 2005. Biogenic particles in the surface microlayer and overlaying atmosphere in the central Arctic Ocean during summer. *Tellus*, **57B,** 305–316.

Lohmann, U. and C. Leck, 2005. Importance of submicrone surface active organic aerosols for pristine Arctic Clouds. *Tellus,* **57B**, 261–268.

Maenhaut W., G. Ducastel, C. Leck, D. Nilsson and J. Heintzenberg, 1996. Multi-elemental composition and sources of the high Arctic atmospheric aerosol during summer and autumn. *Tellus,* **48B**, 300–321.

Mattsson R., J. Paatero and J. Hatakka, 1996. Automatic alpha/beta analyser for air filter samples - absolute determination of radon progeny by pseudo-coincidence techniques. *Radiat. Prot. Dosim.*, **63**, 133–139.

McKinlay, A.F. and B.L. Diffey, 1987. A reference action spectrum for ultraviolet induced erythema in human skin. *CIE J.,* **6**, 17–22.

Meinander, O., A. Kontu, K. Lakkala, A. Heikkilä, L. Ylianttila and M. Toikka, 2008. Diurnal variations in the UV albedo of arctic snow. *Atmos. Chem. Phys*., **8**, 6551–6563.

Nilsson, E.D. and C. Leck, 2002. A pseudo-Lagrangian study of the arctic remote marine sulfur cycle. *Tellus*, **54B**, 213–230.

Orellana M.V. and P. Verdugo, 2003. Ultraviolet radiation blocks the organic carbon exchange between the dissolved phase and the gel phase in the ocean. *Limnol. Oceanogr.* **48**, 1618–1623.

Paatero J., M. Buyukay, V. Aaltonen, M.J. Garcia, R. Sanchéz, J. Hatakka, A. Virkkula A. and K. Teinilä, 2007. Airborne lead-210 at research Aboa and Marambio, Antarctic. In: A.S. Paschoa, A.S. Alencar & R. Amaral (Eds.): Book of Abstracts of the 8th International Symposium on the Natural Radiation Environment (NRE-VIII), Búzios, Rio de Janeiro, 7–12 October 2007. Rio de Janeiro: Natural Radiation Environment Association. p. 65.

Pacyna J. M., E.G. Pacyna and W. Aas, 2009. Changes of emissions and atmospheric deposition of mercury, lead, and cadmium. *Atmos. Environ*., **43**, 117–127.

Papastefanou C. and E.A. Bondietti, 1991. Mean Residence Times of Atmospheric Aerosols in the Boundary Layer as Determined from ^{210}Bi/^{210}Pb Activity Ratios. *J. Aerosol Sci.*, **22**, 927–931.

Perovich D., 2002. Ultraviolet Radiation and the Optical Properties of Sea Ice and Snow. In: Hessen, D. (ed.) 2002, UV Radiation and Arctic Ecosystems, Ecological Studies Vol 153, Springer-Verlag Berlin, Heidelberg.

Pirazzini, R., 2004. Surface albedo measurements over Antarctic sites in summer. *J. Geophys. Res.* **109**, doi:10.1029/2004JD004617.

Preiss N., M.-A. Mélières and M. Pourchet, 1996. A compilation of data on lead 210 concentration in surface air and fluxes at the air-surface and water-sediment interfaces. *J. Geophys. Res.*, **101**, 28847–28862.

Ravindra, K., R. Sokhi and R. Van Grieken, 2008. Review: Atmospheric polycyclic aromatic hydrocarbons: Source attribution, emission factors and regulation. *Atmos. Environ.*, **42**, 2895–2921.

Rolph, G.D., 2003. Real-time Environmental Applications and Display sYstem (READY)

Website (http://www.arl.noaa.gov/ready/hysplit4.html), Silver Spring, MD: NOAA Air Resources Laboratory.

Samuelsson C., L. Hallstadius, B. Persson, R. Hedvall, E. Holm and B. Forkman, 1986. ^{222}Rn and ^{210}Pb in the Arctic Summer Air. *J. Environ. Radioact.,* **3**, 35–54.

Sanak, J., A. Gaudry and G. Lambert, 1981. Size distribution of ^{210}Pb aerosols over oceans. *Geophys. Res. Lett.*, **8**, 1067–1069.

Shevchenko, V., A. Lisitzin, A. Vinogradova and R. Stein, 2003. Heavy metals in aerosols over the seas of the Russian Arctic. *Sci. Tot. Environ.,* **306**, 11–25.

Stebel, K., G. Christensen, J. Derome and I. Grekelä, 2007. State of the Environment in the Norwegian, Finnish and Russian Border Area, The Finnish Environment 6. Finnish Environment Institute, Helsinki.

Suzuki T., Y. Maruyama, N. Nakayama, K. Yamada and K. Ohta, 1999. Measurement of the ^{210}Po/^{210}Pb activity ratio in size fractionated aerosols from the coast of Japan sea. *Atmos. Environ.* **33**, 2285–2288.

Suzuki T., N. Nakayama, M. Igarashi, K. Kamiyama and O. Watanabe, 1996. Concentrations of ^{210}Pb and ^{210}Po in the atmosphere of Ny-Ålesund, Svalbard. *Memoirs of National Institute of Polar Research* **51**, 233–237.

Tjernström, M., M. Žagar, G. Svensson, J.J. Cassano, S. Pfeifer, A. Rinke, K. Wyser, K. Dethloff, C. Jones, T. Semmler and M. Shaw, 2005. Modelling the Arctic boundary layer: An evaluation of six ARCMIP regional-scale models using data from the SHEBA project. *Boundary-Layer Meteor*. **117**: 337–381.

Tjenström, M., J. Sedlar and M. Shupe, 2008. How well do regional climate models reproduce radiation and clouds in the Arctic? An evaluation of ARCMIP simulations. *J. Appl. Meteor. Climat.* **47**: 2405–2422.

Todorovic D., D. Popovic, G. Djuric and M. Radenkovic, 2000. ^{210}Pb in ground-level air in Belgrade city area. *Atmos. Environ.*, **34**, 3245–3248.

Uttal, T., J.A. Curry, M.G. McPhee, D.K. Perovich, R.E. Moritz, J.A. Maslanik, P.S. Guest, H.L Stern, J.A. Moore, R. Turenne, A. Heiberg, M.C. Serreze, D.P. Wylie, O.G.Persson, C.A. Paulson, C. Halle, J.H. Morison, P.A. Wheeler, A. Makstas, H. Welch, M.D. Shupe, J.M. Intrieri, K. Stamnes, R.W. Lindsey, R. Pinkel, W.S. Pegau, T.P. Stanton, and T.C. Grenfeld, 2002: The Surface Heat Budget of the Arctic Ocean. *Bull. Amer. Meteor. Soc.*, **83**, 255–275.

Vaattovaara, P., M. Räsänen, T. Kühn, J. Joutsensaari and A. Laaksonen, 2005. A method for detecting the presence of organic fraction in nucleation mode sized particles. *Atmos. Chem. Phys.* **5**, 3595–3620.

Vaattovaara, P., P.E. Huttunen, Y.J. Yoon, J. Joutsensaari, K.E.J. Lehtinen, C.D. O'Dowd and A. Laaksonen, 2006. The composition of nucleation and Aitken modes particles during coastal nucleation events: evidence for marine secondary organic contribution. *Atmos. Chem. Phys.*, **6**, 4601–4616.

WHO, 2002. Global Solar UV Index: A practical Guide. A joint recommendation of the World Health Organization, World Meteorological Organization, United Nations Environmental Programme, and the International Commission on Non-Ionizing Radiation Protection, World Health Organization. WHO/ASW/OEH/02.2.

Wiedensohler, A., D.S. Covert, E. Swietlicki, P.P. Aalto, J. Heintzenberg and C. Leck, 1996. Occurrence of an ultrafine particle mode less than 20 nm in diameter in the marine boundary layer during Arctic summer and autumn. *Tellus,* **48B**, 213–222.

Wuttke, S., G. Seckmeyer and G. König-Langlo, 2006. Measurements of spectral snow albedo at Neumayer, Antarctica. *Ann. Geophys.,* **24**, 7–21.